MixMo: Mixing Multiple Inputs for Multiple Outputs via Deep Subnetworks

Alexandre Ramé*†1, Rémy Sun*1,2 and Matthieu Cord1,3

¹Sorbonne Université ²Optronics & Missile Electronics, Land & Air Systems, Thales ³Valeo.ai

Abstract

Recent strategies achieved ensembling for free by fitting concurrently diverse subnetworks inside a single base network. The main idea during training is that each subnetwork learns to classify only one of the multiple inputs simultaneously provided. However, the question of how these multiple inputs should be mixed has not been studied yet.

In this paper, we introduce MixMo, a new generalized framework for learning multi-input multi-output deep subnetworks. Our key motivation is to replace the suboptimal summing operation hidden in previous approaches by a more appropriate mixing mechanism. For that purpose, we draw inspiration from successful mixed sample data augmentations. We show that binary mixing in features - particularly with patches from CutMix - enhances results by making subnetworks stronger and more diverse.

We improve state of the art on the CIFAR-100 and Tiny-ImageNet classification datasets. In addition to being easy to implement and adding no cost at inference, our models outperform much costlier data augmented deep ensembles. We open a new line of research complementary to previous works, as we operate in features and better leverage the expressiveness of large networks.

1. Introduction

Convolutional Neural Networks (CNNs) have shown exceptional performances in computer vision tasks such as classification [54]. However, among other limitations, obtaining reliable predictions remains challenging [43, 76]. For additional robustness in real-world scenarios or to win Kaggle competitions, CNNs usually pair up with two practical strategies: data augmentation and ensembling.

Data augmentation reduces overfitting and improves

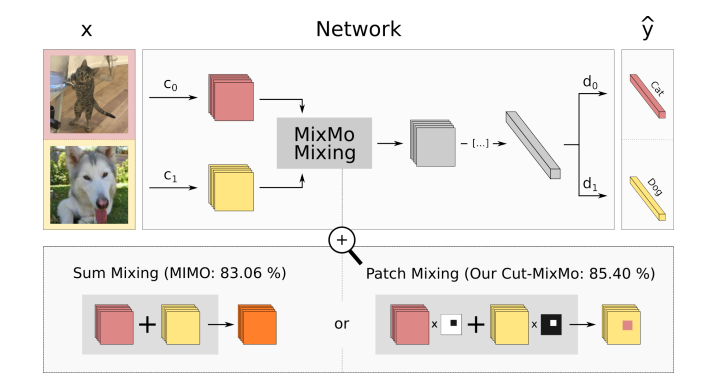


Figure 1: **MixMo overview**. We embed M=2 inputs into a shared space with convolutional layers. The key point of our framework is the subsequent mixing block. In particular, patch mixing surpasses basic summing: 85.40% vs. 83.06% (MIMO [38]) on CIFAR-100 with WRN-28-10.

generalization, notably by diversifying training samples [32]. Traditional image augmentations are label-preserving: e.g flipping, cropping etc [88]. However, recent **mixed** sample data augmentations (MSDA) alter labels: multiple inputs and their labels are mixed proportionally to a ratio λ to create artificial samples. The seminal work Mixup [117] linearly interpolates pixels while Manifold Mixup [101] interpolates latent features in the network. Binary masking MSDAs [27, 37, 53] such as CutMix [114] have since diversified mixed samples by pasting patches from one image onto another in place of interpolation. MSDA have had significant impacts on many successful approaches for fully-[8, 73], semi-[6, 7, 27] and self-[60] supervised learning.

Aggregating predictions from several neural networks significantly improves generalization [20, 36, 56, 110], notably uncertainty estimation [3, 35, 76]. From the Bayesian perspective [39, 108, 109], **model ensembling** reduces variance by averaging a set of diverse predictions. Empirically, an ensemble of several small networks usually performs

^{*}Equal contribution.

[†]Correspondence to alexandre.rame@lip6.fr

better than one large network [15, 67]. Yet unfortunately, ensembling is costly in time and memory, both at training and inference: this often limits applicability.

In this paper, we propose **MixMo**, a generalized multiinput multi-output framework. We remove the inference overhead by fitting $M \geq 2$ independent subnetworks within a single base network [29, 38, 89]. This is possible as networks only leverage a subset of their weights: for example, "winning tickets" [25] subnetworks perform similarly to the full network. Rather than pruning inactive filters [58, 63, 69], we seek to fully use the available neural units.

The challenge is to prevent homogenization and enforce diversity among subnetworks with no structural differences. Thus, we consider M (inputs, labels) pairs simultaneously in training: $\{(x_i,y_i)\}_{0\leq i< M}$. As shown on Fig. 1 with M=2, M images are fed simultaneously. The M inputs are encoded by M separate convolutional layers $\{c_i\}_{0\leq i< M}$ into a shared latent space before being mixed. Then, the representation is fed to the core network, which finally branches out into M dense layers $\{d_i\}_{0\leq i< M}$. Diverse subnetworks naturally emerge as d_i learns to classify y_i from input x_i . At inference, the same image is repeated M times: we obtain ensembling for free by averaging M predictions.

The key divergent point between MixMo variants lies in the **multi-input mixing block**. Should the merging be a basic summation, we would recover an equivalent formulation to MIMO [38], that first featured this multi-input multi-output strategy. Contrarily to classical fusion mechanisms that detect tensors' intercorrelations [5, 11], we seek features independence. This makes summing suboptimal.

Our main intuition is simple: we see summing as a restrictive and balanced form of Mixup [117] where $\lambda = \frac{1}{M}$. By analogy, we draw from the considerable MSDA literature to design a more appropriate mixing block. In particular, we leverage binary masking methods to ensure subnetworks diversity. Our framework empowers us to innovate and create a new Cut-MixMo, inspired by CutMix [114] and illustrated in Fig. 1: a patch of features from the first input is pasted into the features from the second input. This asymmetrical mixing also raises new questions regarding information flow in the network's features: we tackle the imbalance between the multiple classification training tasks via a new weighting scheme.

In summary, our contributions are threefold:

- 1. We propose a general framework, MixMo, connecting two successful fields: mixing samples data augmentations & multi-input multi-output ensembling.
- We identify the appropriate mixing block to best tackle the diversity/individual accuracy trade-off in subnetworks: the easy to implement Cut-MixMo benefits from the synergy between CutMix and ensembling.

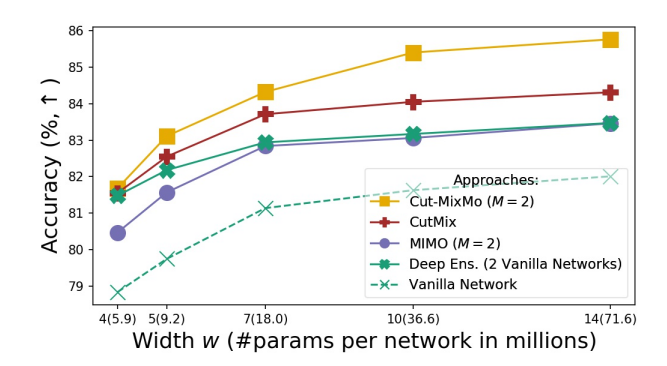


Figure 2: **Main results**. CIFAR-100 with WRN-28-w. Cut-MixMo variant (patch mixing and M=2) defeats CutMix and deep ensembles (despite half the parameters) by leveraging over-parametrization in wide networks.

3. We design a new weighting of the loss components to properly leverage the asymmetrical inputs mixing.

We demonstrate excellent accuracy and uncertainty estimation with MixMo on standard datasets CIFAR-10/100 and Tiny ImageNet. As exhibited by Fig. 2, Cut-MixMo with M=2 outperforms CutMix, MIMO and deep ensembles, at (almost) the same inference cost as a single network.

2. Related work

2.1. Data augmentation

CNNs are known to memorize the training data [116] and to make overconfident predictions [33] to the detriment of generalization. **Data Augmentations** (DA) increase the training dataset's size by creating artificial samples from available labeled data. Beyond slight perturbations, Aug-Mix [44], recently increased amplitudes [42] to improve robustness [43]. CutOut [19] randomly deleted regions of images in training to prevent models from focusing on a single region, similarly to how regularizations like Dropout [91] or DropBlock [31] force networks to leverage latent features.

Mixed Sample Data Augmentation (MSDA) recently expanded the notion of DA. From pairs of labeled samples $\{(x_i,y_i),(x_k,y_k)\}$, they create virtual samples: $(m_x(x_i,x_k,\lambda),\lambda y_i+(1-\lambda)y_k)$ where $\lambda \sim \text{Beta}(\alpha,\alpha)$. [64] showed that mixing the targets differently than this linear interpolation may cause underfitting and unstable learning. Indeed, approaches mainly focused on developing the most effective input mixing m_x . In [48, 97, 98, 117], m_x performs a simple linear interpolation between pixels: e.g in Mixup [117], $m_x(x_i,x_k,\lambda) = \lambda x_i + (1-\lambda)x_k$. It regularizes outside the empirical training distribution [34, 118].

CutMix draws from Mixup [117] and CutOut [19] by pasting a patch from x_k onto x_i . $m_x(x_i, x_k, \lambda) = \mathbb{1}_m \odot x_i + (\mathbb{1} - \mathbb{1}_m) \odot x_k$ where \odot represents the element-wise prod-

uct and $\mathbb{1}_m$ is a randomly chosen binary mask with average value λ and valued at 1 on a rectangle. Such **non-linear binary masking** improves generalization [92, 95] by dramatically increasing dataset diversity: it creates new images with usually mutually exclusive features [37]. [4, 23, 59] sought more diverse transformations via arbitrarily shaped binary masks: proposals range from cow-spotted [26, 27] to masks with irregular edges [37]. As masking of discriminative regions may cause label misallocation [34], [17, 52, 53, 51, 100, 102] tried to leverage costly saliency heatmaps [85]: yet, recent ResizeMix [81] showed that they perform no better than random selection of patch locations.

A few works [23, 62, 112, 114] mixed intermediate **latent features** so that both samples provide relevant content. In particular, Manifold Mixup [101] successfully extended Pixels Mixup [117]. As shown later, the main drawbacks compared to MixMo are that they encode both inputs with the same encoder and have only one classifier.

2.2. Ensembling

Aggregating predictions from multiple models is a standard trick in machine learning [20, 36, 55, 72, 84]. Ideally, members should be both *accurate* and *diverse* [74, 80, 82]. Deep ensembles [56] (DE) simultaneously train multiple networks with different random initializations converging towards different explanations for the training data [24, 109]. Diversity may be further strengthened [77, 82, 106] at the risk of reducing individual performances.

Ensembling's fundamental drawback is the inherent computational and memory overhead, which increases linearly with the number of members. This bottleneck is typically addressed by sacrificing either individual performance or diversity in a complex trade-off. Averaging predictions from several checkpoints on the training process, *i.e.* snapshot ensembles [30, 47, 49, 68, 83, 111, 119], fails to explore multiple local optima [3, 24, 109]. So does Monte Carlo Dropout [28]. The recent BatchEnsemble [22, 107] is parameter-efficient, yet still requires multiple forward passes. TreeNets [61, 75, 87, 94] reduce training and inference cost by sharing low-level layers among members. MotherNets [104] share first training epochs between members. However, sharing reduces diversity. The knowledge from the whole ensemble may be distilled into a single member, via online [14, 57, 90] or offline [66, 99] distillation [10, 45]: yet, it reduces performances.

Very recently, the multi-input multi-output MIMO [38] achieves **ensemble almost for free**: all of the layers except the first convolutional and last dense layers are shared ($\approx +1\%$ #parameters). [89] motivated a related Aggregated Learning to learn concise representations with arguments from information bottleneck [2, 96]. The idea is that over-parameterized CNNs [25, 70, 79, 121] can fit multiple subnetworks. The question is how to prevent homog-

enization among the simultaneously trained subnetworks. Facing a similar challenge, [29] included stochastic channel recombination, [21] relied on predefined binary masks: in GradAug [113], subnetworks only leverage the first channels up to a given percentage. In contrast, MIMO does not need structural differences among subnetworks: they learn to build their own paths while being as diverse as in DE.

3. Model

We first introduce our framework MixMo for mixing multiple inputs for multiple outputs via subnetworks, summarized in Fig. 3. After having highlighting our key mixing block that combines information from inputs, we motivate our training loss. Reversely, we analyze MixMo as a new data augmentation with multiple encoders and decoders.

We mainly study M=2 subnetworks, for improved clarity and as it empirically performs best in standard parameterization regimes. For completeness, we straightforwardly generalize to M>2 in Section 3.5.

3.1. MixMo framework

We leverage a training classification **dataset** D of i.i.d. pairs of associated image/label $\{x_i, y_i\}_{i=1}^{|D|}$. We randomly sample a subset of |B| samples $\{x_i, y_i\}_{i \in B}$ that we randomly shuffle via π . Our training batch is $\{(x_i, x_j), (y_i, y_j)\}_{i \in B, j = \pi(i)}$. The loss $\mathcal{L}_{\text{MixMo}}$ is averaged over these |B| samples: the networks' weights are updated through backpropagation and gradient descent.

Let's focus on the training sample $\{(x_0, x_1), (y_0, y_1)\}$. In MixMo, both inputs are **separately encoded** (see Fig. 1 into the shared latent space with 2 different convolutional layers (with 3 input channels each and no bias term): x_0 via c_0 and x_1 via c_1 . To recover a strict equivalent formulation to MIMO [38], we simply sum the 2 encodings: $c_0(x_0) + c_1(x_1)$. Indeed, MIMO merged inputs through channel-wise concatenation in pixels: MIMO first convolutional layer (with 6 input channels and no bias term) hides the summing operation in the output channels.

Explicitly highlighting the underlying mixing procedure leads us to consider a **general multi-input mixing block** \mathcal{M} . This manifold mixing presents a unique opportunity to tackle the ensemble diversity/individual accuracy tradeoff and to improve overall ensemble results (see Section 3.2). The shared representation $\mathcal{M}(c_0(x_0), c_1(x_1))$ feeds the next convolutional layers. We note κ the mixing ratio.

The core network \mathcal{C} extracts features that represent both inputs simultaneously. Dense layer d_0 predicts $\hat{y}_0 = d_0 \left[\mathcal{C} \left(\mathcal{M} \left\{ c_0(x_0), c_1(x_1) \right\} \right) \right]$ and targets y_0 , while d_1 targets y_1 . Thus, the **training loss** is the sum of 2 cross-entropy \mathcal{L}_{CE} , weighted by parametrized function w_r (defined in Section 3.3) to balance the asymmetry when $\kappa \neq 0.5$:

$$\mathcal{L}_{\text{MixMo}} = w_r(\kappa) \mathcal{L}_{\text{CE}}(y_0, \hat{y}_0) + w_r(1-\kappa) \mathcal{L}_{\text{CE}}(y_1, \hat{y}_1).$$
 (1)

At inference, the same input x is repeated twice: core network $\mathcal C$ is fed the sum $c_0(x)+c_1(x)$ that preserves maximum information from both encodings. Then, we average both diverse predictions: $\frac{1}{2}\left(\hat{y}_0+\hat{y}_1\right)$. The whole point of this is to benefit from ensembling in a single forward pass.

3.2. Mixing block \mathcal{M}

The mixing block \mathcal{M} - which combines both inputs into a shared representation - is the cornerstone of MixMo. Our generalized framework encompasses a wide range of variants inspired by MSDA mixing methods. In particular, we analyze MIMO as a simplified MixUp variant where the mixing ratio κ is fixed to 0.5. In this paper, we mainly focus around the more effective **Cut-MixMo** variant:

$$\mathcal{M}_{\text{Cut-MixMo}}(l_0, l_1) = 2 \left[\mathbb{1}_{\mathcal{M}} \odot l_0 + (\mathbb{1} - \mathbb{1}_{\mathcal{M}}) \odot l_1 \right], \quad (2)$$

where $l_0=c_0(x_0),\, l_1=c_1(x_1),\, \mathbb{1}_{\mathcal{M}}$ is a binary mask with area ratio $\kappa\sim \operatorname{Beta}(\alpha,\alpha)$, valued at 1 either on a rectangle either on the complementary of a rectangle. In other words, a patch from $c_0(x_0)$ is incorporated into $c_1(x_1)$, or vice versa. Cut-MixMo performs slightly better than more complex binary mixing (see Section 4.3.2), and significantly better than Linear-MixMo that extends Mixup, $\mathcal{M}_{\operatorname{Linear-MixMo}}(l_0,l_1)=2\left[\kappa l_0+(1-\kappa)l_1\right]$. We now argue that binary masking advantageously replaces linear interpolation: subnetworks are more accurate and more diverse.

First, binary mixing in \mathcal{M} trains stronger **individual** subnetworks for the same reasons why CutMix improved over Mixup. In a nutshell, linear MSDA [101, 117] produce noisy samples [12] that lead to robust representations. As MixMo tends to distribute different inputs on nonoverlapping channels (as discussed later in Fig. 4a), this regularization hardly takes place anymore in $\mathcal{M}_{\text{Linear-MixMo}}$. On the contrary, by masking features, we simulate common object occlusion problems. This spreads subnetworks' focus across different locations: the 2 classifiers are forced to find information relevant to their assigned input at disjoint locations. Note that this occlusion remains effective as the receptive field in this first shallow latent space remains small.

Secondly, linear interpolation is fundamentally ill-suited to induce diversity as full information is preserved from both inputs. CutMix on the other hand explicitly increases dataset diversity by presenting patches of images that do not normally appear together. Such benefits can be directly transposed to $\mathcal{M}_{\text{Cut-MixMo}}$: binary mixing with patches increases randomness and **diversity between the subnetworks**. Indeed, in a similar spirit to bagging [9], different samples are given to the subnetworks. By deleting asymmetrical complementary locations from the two inputs, subnetworks will not rely on the same region and information. Overall, they are less likely to collapse on close solutions.

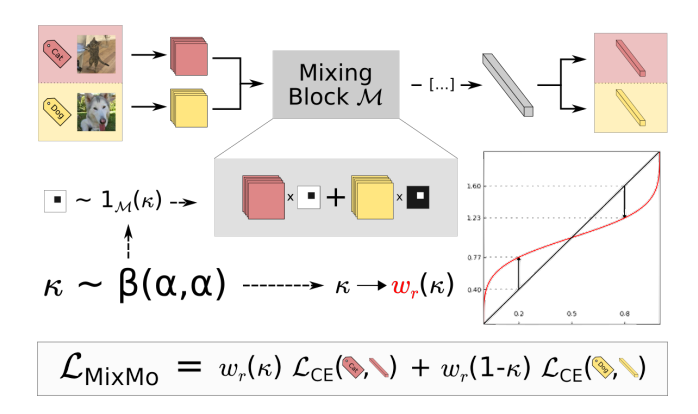


Figure 3: **MixMo learning components**. The asymmetry in mixing influences the balance of the training loss.

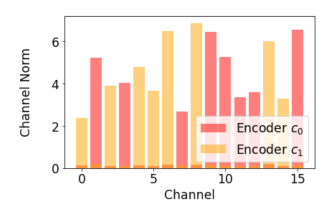
3.3. Loss weighting w_r

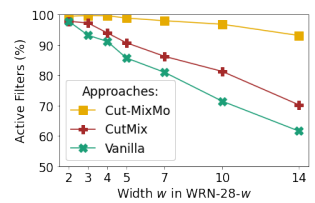
Asymmetries in the mixing mechanism can cause one input to overshadow the other. Notably when $\kappa \neq 0.5$, the predominant input may be easier to predict. We seek a weighting function w_r to balance the relative importance of the two \mathcal{L}_{CE} in \mathcal{L}_{MixMo} . It modifies the effective learning rate, how gradient flows in the network and overall how mixed information is represented in features. Interestingly, this is a central theme in **multi-task learning** [13]: while it aims at predicting several tasks from a shared input, we predict a shared task from several different inputs. Beyond this chiastic structure, we face similar issues. In particular, information separation from a shared representation is challenging. Moreover, gradients for one task can be detrimental to another conflicting task [50, 86, 93]. Fortunately, MixMo presents a distinct advantage: the exact ratios κ and $1 - \kappa$ of each task are known exactly.

We therefore leverage κ to weight via:

$$w_r(\kappa) = 2 \frac{\kappa^{1/r}}{\kappa^{1/r} + (1-\kappa)^{1/r}}.$$
 (3)

This defines a family of functions by varying the parameter r, visualized for r=3 in red in Fig. 3 (more in Appendix 6.1). This power law provides a natural relaxation between **two extreme configurations**. The first extreme, $r=1, w_1(\kappa)=2\kappa$, is in line with linear label interpolation in MSDA. The resulting imbalance in each subnetwork's contribution to $\mathcal{L}_{\text{MixMo}}$ causes lopsided updates. While it promotes diversity, it also reduces regularization: the overshadowed input has a reduced impact on the loss. The opposite extreme, $r\to\infty, w_\infty(\kappa)\to 1$, removes reweighting. Consequently, w_r inflates the importance of hard minority inputs, à la Focal Loss [65]. However, minimizing the role of the predominant inputs destabilize training. Overall, we empirically observe that in-between r perform best as they trade off pros and cons from both extremes.





- (a) Filters l_1 -norms of the input encoders c_0 and c_1 .
- (b) Proportion of active filters in core network vs. width w.

Figure 4: Influence of MixMo on network utilization. (a) The encoders have separated channels: the two subsequent classifiers can differentiate the two inputs. (b) Less filters are strongly active $(\|f_i\|_1 \ge 0.4 \times \max_{f \in layer} \|f\|_1)$ in wider networks: Cut-MixMo reduces this negative point.

3.4. From manifold MSDA to MixMo

We have discussed at length how we extend multi-input multi-output frameworks by borrowing mixing protocols from MSDA. Now we flip the script and point out how our **MixMo diverges from MSDA schemes**. At first glimpse, the idea is the same as manifold mixing [23, 62, 101, 114]: M=2 inputs are encoded into a latent space to be mixed before being fed to the rest of the network. In addition to our mixing being shallower, there are two key differences: *first*, MixMo uses 2 different encoders (one for each input), and *second*, it outputs 2 predictions instead of a single one.

Indeed, MSDA have a single prediction head that targets a unique soft label: it reflects the different classes via linear interpolation. MixMo instead chooses to fully leverage the composite nature of mixed samples and trains **separate dense layers**, d_0 and d_1 , ensembled for free at test time.

Section 4.3.5 shows that this only works because MixMo also uses 2 **different encoders** c_0 and c_1 . While training 2 classifiers may seem straightforward in MSDA, it actually raises a troubling question: which input should each predictor classifies? Having 2 different encoders provides a simple solution: the network is divided in two subnetworks - one for each input. Their separability is easily observed: e.g. Fig. 4a shows the l_1 -norm of the 16 channels for the two encoders (WRN-28-10 on CIFAR-100). Each channel norm is far from zero in only one of the two encoders: thus, $c_0(x_0)$ and $c_1(x_1)$ do not overlap much in the mixing space and will be treated differently by the subsequent layers.

This leads MixMo to use most available filters. Taking a page out of the structured pruning literature [63], we consider in Fig. 4b that a filter (in a layer of the core network) is active if its l_1 -norm is at least 40% of the l_1 -norm from its layer's most active filter (see Appendix 6.2). This proportion of active filters decreases with width w: vanilla and CutMix networks do to fully use additional parameters. In contrast, MixMo better leverages over-parameterization thanks to its 2 encoders, decoders and subnetworks.

3.5. Generalization to $M \ge 2$ subnetworks

Most of the framework is easily extended by optimizing $\mathcal{L}_{\text{MixMo}} = \sum_{0 \leq i < M} M \frac{\kappa_i^{1/r}}{\sum_j \kappa_j^{1/r}} \mathcal{L}_{\text{CE}}\left(y_i, \hat{y}_i\right)$ with $\left\{\kappa_i\right\} \sim \text{Dir}(\alpha)$ dirichlet distribution. See details in Appendix 6.3. The key change is that \mathcal{M} now needs to handle more than 2 inputs: $\{c_i(x_i)\}_{0 \leq i < M}$. While linear interpolation is easily generalized, Cut-MixMo has several possible extensions: in our experiments, we first linearly interpolates between M-1 inputs and then patch a region from the M-th.

4. Experiments

We now evaluate the efficacy of our approach on standard image classification datasets: CIFAR-{10, 100} [54] with WRN-28-{2,3,4,5,7,10,14} [115] architectures and Tiny ImageNet [16] with PreActResNet-18-{1,2,3} [41].

We equally track classification accuracies (Top{1,5}, \uparrow) and the *calibrated Negative Log-Likelihood* (NLL_c, \downarrow). Indeed, [3] showed that we should compare in-domain uncertainty estimations after temperature scaling [33]: thus we split the test set in two and calibrate (after averaging in ensembles) with the temperature optimized on the other half. **Bold** highlights best scores, \dagger marks not reproduced papers.

4.1. Implementation details

We mostly study the strong Cut-MixMo variant with $M{=}2$. For the **hyper-parameters**, we set $r{=}3$ (see Expe. 4.3.3). $\alpha{=}2$ performs better than 1 (see Appendix 6.7). In contrast, MIMO [38] refers to linear summing, like Linear-MixMo, but with $\kappa{=}0.5$ instead of $\kappa \sim \text{Beta}(\alpha, \alpha)$. We provide more details in Appendix 6.4 and will open source our PyTorch [78] implementation.

Different mixing methods can create a strong **train-test** distribution shift [12, 32]. Thus in practice we substitute $\mathcal{M}_{\text{Cut-MixMo}}$ for $\mathcal{M}_{\text{Linear-MixMo}}$ with probability 1-p to accommodate for the behavior in inference (where we mix via summing to preserve information). We set $p{=}0.5$ with linear descent to 0 over the last training epochs.

When MixMo is combined with MSDA in pixels such as CutMix, the inputs may be of the form: $(m_x(x_i, x_k, \lambda), m_x(x_j, x_{k'}, \lambda'))$, where x_k and $x_{k'}$ are randomly chosen in the whole dataset and $\lambda, \lambda' \sim \text{Beta}(1)$.

MIMO duplicates samples b times via **batch repetition**: x_i will be associated with $x_{\pi(i)}$ and $x_{\pi'(i)}$ in the same batch if $b{=}2$. As the batch size remains fixed, the count of unique samples per batch and the learning rate is divided by b. Conversely, the number of steps is multiplied by b. Overall, this stabilizes training but multiplies its cost by b. Thus we indicate an estimated (training/inference) overhead (wrt. vanilla training) in the *time* column of our tables. Note that some concurrent approaches also lengthen training: e.g. GradAug [113] via multiple subnetworks predictions ($\approx \times 3$).

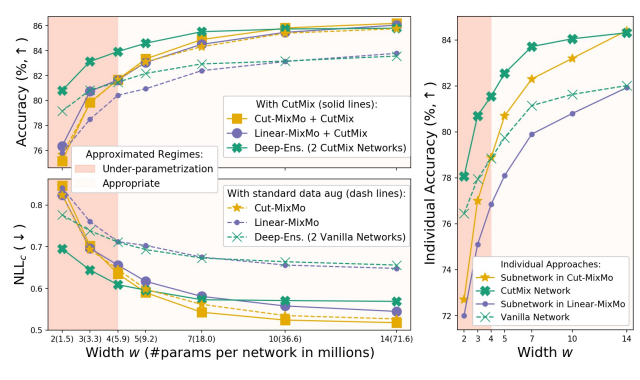
4.2. Main results on CIFAR-100 and CIFAR-10

Tab. 1 reports averaged scores over 3 runs for our main experiment on CIFAR with WRN-28-10. We reuse the hyper-parameters given in MIMO [38]. **Cut-MixMo** reaches (85.40% Top1, 0.535 NLL $_c$) on CIFAR-100 with b=4: it surpasses Linear-MixMo (83.08%, 65.6) and MIMO (83.06%, 0.661). Crucially, Cut-MixMo **benefits from CutMix** (85.77%, 0.524) and outperforms the competitive DE with 2 CutMix networks (85.74%, 0.574). Performances remain strong when b=2: sole Cut-MixMo (84.38%, 0.563) proves better than previous MSDA like Puzzle-Mix [53] or CutMix. We obtain similar conclusions on CIFAR-10, with the longer batch augmented Mixup BA [46] barely edging out. Yet, Cut-MixMo best estimates uncertainty (0.079 NLL $_c$), even without CutMix (0.081).

Fig. 5 shows how Cut-MixMo grows stronger than standard methods as width w in WRN-28-w increases. The parameterization becomes appropriate at w=4: Cut-MixMo (yellow curves) matches DE (with half the parameters) in Fig. 5a and its subnetworks match a vanilla network in Fig. 5b. Cut-MixMo better uses additional parameters: at w \ge 10 (resp. w>5), Cut-MixMo+CutMix surpasses DE+CutMix in Top1 (resp. in NLL $_c$). Compared to our already strong Linear-MixMo+CutMix, Cut-MixMo performs similarly in Top1, and even surpasses it with CutMix for w \ge 4. Critically, Cut-MixMo, even without CutMix, is significantly better in NLL $_c$. Overall, binary mixing advantages cannot be fully compensated by data augmentations.

Table 1: Main results: WRN-28-10 on CIFAR.

Dataset	Dataset		IFAR-10	CIFAR-10		
Approach	Time Tr./Inf.	Top1 %	Top5	$\begin{array}{c} \mathrm{NLL}_c \\ 10^{-2} \end{array}$	Top1 %	$\begin{array}{c} \mathrm{NLL}_c \\ 10^{-2} \end{array}$
Vanilla Mixup ManMixup [†] CutMix CowMix ResizeMix [†]	1/1	81.63 83.44 81.96 84.05 83.53 84.31	95.49 95.92 - 96.09 95.94	73.9 65.7 - 64.8 66.5	96.34 97.07 97.45 97.23 97.35 97.60	12.6 11.2 - 9.9 9.6
Puzzle-Mix [†]	2/1	84.31	96.46	66.8	-	-
GradAug† + CutMix†	3/1	84.14 85.51	96.43 96.86	-	-	-
Mixup BA [†]	8/1	84.30	-	-	97.80	-
DE (2 Nets) + CutMix	2/2	83.17 85.74	96.37 96.82	66.4 57.1	96.67 97.52	11.1 8.6
MIMO		82.40	95.78	68.8	96.38	12.1
Linear-MixMo + CutMix	2/1	82.54 84.69	95.99 97.12	67.6 57.2	96.56 97.32	11.4 9.4
Cut-MixMo + CutMix		84.38 85.18	96.94 97.20	56.3 54.5	97.31 97.45	8.9 8.4
MIMO		83.06	96.23	66.1	96.74	11.4
Linear-MixMo + CutMix	4/1	83.08 85.47	96.26 97.04	65.6 55.8	96.91 97.68	10.8 8.7
Cut-MixMo + CutMix		85.40 85.77	97.22 97.42	53.5 52.4	97.51 97.73	8.1 7.9



- (a) Ensemble Top1 and NLL_c.
- (b) Individual Top1.

Figure 5: **Parameters efficiency** (metrics/#params). CIFAR-100 with WRN-28-w, b=4. Comparisons between ensemble (a) and some of their individual (b) counterparts.

4.3. MixMo variants on CIFAR-100 w/ WRN-28-10

4.3.1 Training time analysis

In Fig. 6, we lengthen training with batch repetition b for MixMo approaches, or with multiple networks N for DE: b and $N \in \{1,2,4\}$. Indeed, MixMo with batch repetition set to $b{=}4$ matches the training time of DE with $N{=}4$ networks. Cut-MixMo outperforms Linear-MixMo and even DE (without the inference overhead) at same training time in all setups. In the remainder of this section, we set $b{=}2$.

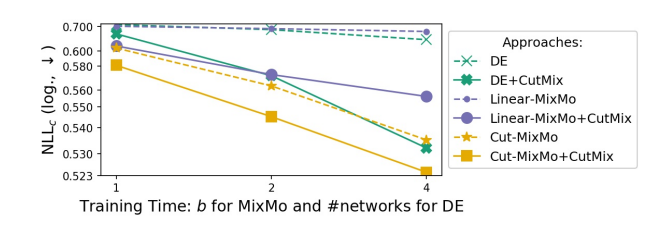


Figure 6: $NLL_c(\downarrow)$ improves with longer train, through batch repetitions (MixMo) or additional networks (DE).

4.3.2 The mixing block \mathcal{M}

Tab. 2 compares performances for several mixing blocks [23, 37, 92, 114]. No matter the **shape** (illustrated in Appendix 6.6), binary masks perform better than linear mixing: the cow-spotted mask (84.17%, 0.561) [26, 27] notably performs well. The basic CutMix patching (84.38%, 0.563) is nevertheless more accurate and was our main focus.

Table 2: \mathcal{M} inspired by various **MSDA approaches**.

\mathcal{M} approach	Mixup [117]	Horiz. Concat.	Vertical Concat.	PatchUp 2D [23]	FMix [37]	CowMix [26, 27]	CutMix [114]
Top1 NLL_c	82.5 0.676	82.78 0.627	84.00 0.573	84.16 0.581	83.76 0.602	84.17 0.561	84.38 0.563

We further study the impact of binary mixing through the lens of the *ensemble diversity/individual accuracy trade off*. Following [82], we measure diversity via the ratio-error [1] (d_{re}, \uparrow) , defined as the ratio between the number of different errors and of simultaneous errors for a pair of predictors. In Fig. 7 and 8, we average metrics over the last 10 epochs.

Fig. 7 (and Appendix 6.5) supports our claim that patch mixing increases diversity compared to linear mixing: as the probability p of patch mixing grows, so does diversity: from $d_{re}(p{=}0.0)\approx 0.78$ (Linear-MixMo) to $d_{re}(p{=}0.5)\approx 0.85$ (Cut-MixMo). In contrast, DE have $d_{re}\approx 0.76$ on this setup. Beyond adding randomness, masking forces the subnetworks to look at disjoint areas. Setting p past 0.6 increases diversity even higher, though at the cost of subnetworks accuracies. This is due to underfitting and increased test-train distribution gap. Thus $p\in[0.5,0.6]$ best trade off.

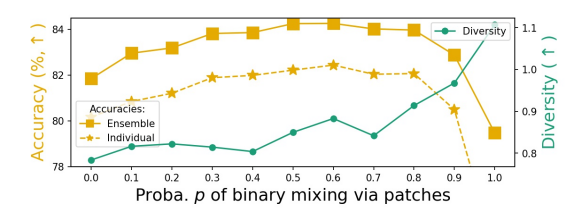


Figure 7: **Diversity/accuracy** as function of p with r=3.

4.3.3 Weighting function w_r

Higher values of r in w_r tend to remove reweighting, as shown in Appendix 6.1: they strongly decrease diversity in Fig. 8. The opposite extreme with $r{=}1$ increases diversity via lopsided gradient updates: yet, it degrades individual accuracy. We speculate it underemphasizes hard samples. On the intermediate range $r \in [3,6]$, results remain high and stable as Cut-MixMo strikes good balance.

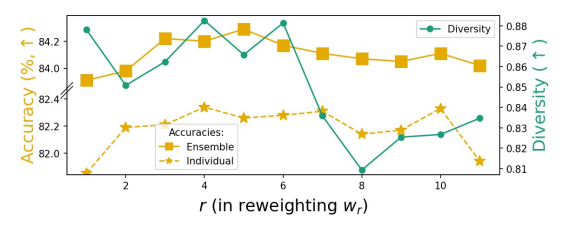


Figure 8: **Diversity/accuracy** as function of r with p=0.5.

4.3.4 Generalization to $M \geq 2$ subnetworks

In Fig. 9, Cut-MixMo's subnetworks perform at 82.3% when $M{=}2$ vs. 79.5% when $M{=}3$. In MIMO, it's 79.8% vs. 77.7%. Because subnetworks do not share features, higher M degrades their performances: only two can fit seamlessly. Overall, ensemble Top1 decreases in spite of the additional predictions, as already noticed in MIMO [38].

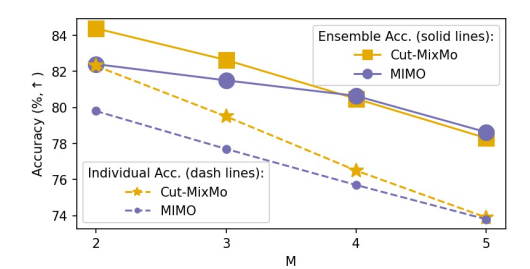


Figure 9: Ensemble/individual accuracies for $M \geq 2$.

This reflects MixMo's strength in over-parametrized regimes, but also its limits with fewer parameters when subnetworks underfit (recall previous Fig. 5). Facing similar findings, MIMO [38] introduced input repetition so that subnetworks share their features, at the cost of drastically reduced diversity. Our generalization may be extended by future approaches whose mixing blocks (perhaps not inspired by MSDA) would hopefully tackle these issues.

4.3.5 Multiple encoders and classifiers

In Section 3.4, we compared MixMo and MSDA: Tab. 3 confirms the need of **2 encoders and 2 classifiers**. With 1 classifier and linearly interpolated labels as in MSDA, the 2 encoders collapse and perform worse than 1 encoder. With 1 shared encoder and 2 classifiers, it's not clear

Table 3: Number of encoders/classifiers.

# Enc.	# Clas.	$ $ NLL $_c$
1	1	0.604
2	1	0.666
1	2⊖	0.687
1	2^{\otimes}	0.598
2	2	0.563

which input each classifier should target. In the first naive \ominus , we randomly associate the 2 classifiers and the 2 inputs (encoded with the same encoder). This \ominus variant yields poor results. In \otimes , the first classifier tries to predict the label from the predominant input, the second targets the minority input: \otimes reaches 0.598 vs. 0.563 for the full Cut-MixMo.

4.4. Robustness to image corruptions

Deep networks' performances decrease when facing unfamiliar samples. To measure robustness to train-test distribution gap, [43] corrupted CIFAR-100 test images into CIFAR-100-c. We follow Puzzle-Mix [53] and report results with and without AugMix [44], a pixels data augmentation technique specifically introduced to tackle this task. More details in Appendix. In Tab. 4, Cut-MixMo best complements AugMix (71.1% Top1, 89.5% Top5), notably by surpassing the strong DE trained with AugMix as in [105].

Table 4: **WRN-28-10 on CIFAR-100-c**. (b=4).

		CutMix										
AugMix	-	✓	-	-	✓	-	✓	-	-	✓	-	✓
			51.93								56.9	71.1
Top5	73.7	87.5	72.03	77.3	87.7	74.9	88.9	74.9	76.1	89.4	77.2	89.5

4.5. Scaling to Tiny ImageNet

At a larger scale and with more varied images, Cut-MixMo reaches a new state of the art of 70.24% on Tiny ImageNet [16] in Tab. 5. We re-use the hyper-parameters given in previous state of the art Puzzle-Mix [53].

With w=1, PreActResNet-18 is not sufficiently parametrized for MixMo's advantages to express themselves on this challenging dataset. MixMo's full potential shines with wider networks: with w=2 and 44.9M parameters, Cut-MixMo reaches (69.13%, 1.28) vs. (67.76%, 1.33) for CutMix. Compared to DE with 3 networks, Cut-MixMo performs {worse, similarly, better} for $w \in \{1,2,3\}$. At (almost) same numbers of parameters, Cut-MixMo when w=2 performs better (69.13%, 1.28) than DE with 4 networks when w=1 (67.51%, 1.31).

Table 5: **Results**: PreActResNet-18-w on Tiny ImageNet.

Width w (# pa	rams)	w=1	$1 (11.2M) \mid w = 2 (44.9M)$			w = 3 (100.5M)		
Approach	Time Tr./Inf.	Top1	NLL_c	Top1	NLL_c	Top1	NLL_c	
Vanilla Mixup ManMixup [†] CutMix	1/1	62.56 63.74 58.70 65.09	1.53 1.62 - 1.58	64.80 66.62 - 67.76	1.51 1.50 - 1.33	65.78 67.27 - 68.95	1.53 1.51 - 1.29	
Puzzle-Mix [†]	2/1	64.48	1.65	-	-	-	-	
DE (2 Nets) DE (3 Nets) DE (4 Nets)	2/2 3/3 4/4	65.53 66.76 67.51	1.39 1.34 1.31	68.06 69.05 69.94	1.37 1.29 1.24	68.38 69.36 69.72	1.36 1.28 1.26	
Linear-MixMo Cut-MixMo	2/1	61.58	1.61 1.48	66.62	1.41 1.30	68.18 69.89	1.36 1.26	
Linear-MixMo Cut-MixMo	4/1	62.91 64.44	1.51 1.48	67.03 69.13	1.41 1.28	68.38 70.24	1.38 1.19	

4.6. Ensemble of MixMo

Since MixMo adds very little parameters ($\approx +1\%$), we can combine independently trained MixMo like in DE. This ensembling of ensemble of subnetworks leads in practice to the averaging of $M\times N=2\times N$ predictions. Fig. 10 compares ensembling for vanilla networks and Cut-MixMo on CIFAR-100. We first recover the Memory Split Advantage [15, 67, 103, 120] (MSA): at similar parameters count, N=5 vanillas WRN-28-3 do better than a single vanilla WRN-28-7 (+0.10 in NLL_c). Cut-MixMo challenges this MSA: we bridge the gap between using one network or several smaller networks (-0.04 on same setup). Visually, Cut-MixMo's curves remain closer to the lower envelope: performances are less dependent on how the memory budget is split. This is because Cut-MixMo is effective mainly for larger architectures by better using their parameters.

We also recover that vanilla wide networks tend to be less diverse [71], and thus to gain less from ensembling [67]: N=2 vanillas WRN-28-14 (83.47% Top1,

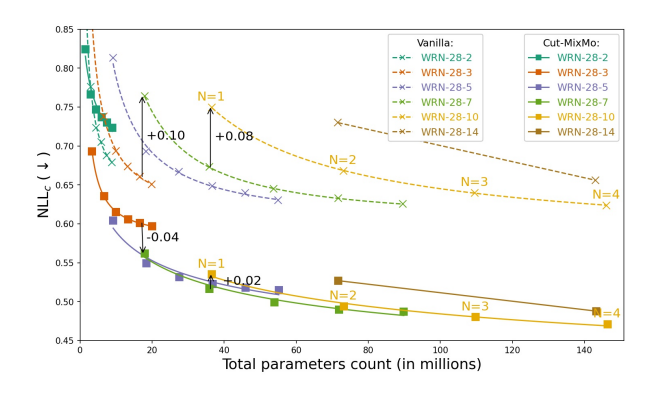


Figure 10: **Ensemble effectiveness** (NLL_c/#params). We slide the width in WRN-28-w and numbers of members N. Standard data augmentations on CIFAR-100. Interpolations through power laws [67].

 $0.656~\rm NLL_c)$ perform not much better than $N{=}2~\rm WRN{-}28{-}7~(82.94\%,\,0.673)$. Contrarily, **Cut-MixMo facilitates the ensembling of large networks** with (86.58%, 0.488) vs. (85.50%, 0.516) (more comparisons in Appendix 6.8). When combined with CutMix [114], Cut-MixMo previously set a new state of the art of 85.77% with $N{=}1~\rm WRN{-}28{-}10$. Tab. 6 shows it further reaches 86.81% with $N{=}3$.

Table 6: **Best results for WRN-28-10 on CIFAR-100** via Cut-MixMo + CutMix [114] + N-ensembling and b=4. Recent Top1 SoTAs: 85.23 [81], 85.51 [113], 85.74 [120].

	#		Average			Best run	
1 V	# params	Top1	Top5	NLL_c	Top1	Top5	NLL_c
1	36.6M	85.77 ± 0.14	97.36 ± 0.02	0.524 ± 0.005	85.92	97.36	0.518
2	73.2M	86.63 ± 0.19	97.73 ± 0.05	0.479 ± 0.003	86.75	97.80	0.475
3	109.8M	86.81 ± 0.17	97.85 ± 0.04	0.464 ± 0.002	86.94	97.83	0.464

5. Conclusion

We generalize the multi-input multi-output strategy and draw inspiration from recent data augmentations to design the appropriate mixing block. That is why MixMo can be analyzed either as an ensembling method or a new mixed samples data augmentation, while still remaining complementary to works from both lines of research. We balance the training procedure with a new weighting scheme. Overall, we demonstrated that our new framework MixMo strongly improves performance. In particular, the Cut-MixMo variant improves the state of the art on CIFAR-100, CIFAR-100-c and Tiny ImageNet.

MixMo better utilizes large networks capacity and may become an important tool for real world projects. We hope to see the framework components evolve to tackle new problems in future works. For instance, it will be interesting to see how the mixing block may be adapted to tasks beyond vision such as natural language processing.

Acknowledgments

This work was granted access to the HPC resources of IDRIS under the allocation 20XX-AD011012262 made by GENCI. We acknowledge the financial support by the ANR agency in the chair VISA-DEEP (project number ANR-20-CHIA-0022-01).

References

- [1] Matti Aksela. Comparison of classifier selection methods for improving committee performance. In *International Workshop on Multiple Classifier Systems*, pages 84–93. Springer, 2003.
- [2] Alex Alemi, Ian Fischer, Josh Dillon, and Kevin Murphy. Deep variational information bottleneck. In *In International Conference on Learning Representations*, 2017.
- [3] Arsenii Ashukha, Alexander Lyzhov, Dmitry Molchanov, and Dmitry Vetrov. Pitfalls of in-domain uncertainty estimation and ensembling in deep learning. In *International Conference on Learning Representations*, 2020.
- [4] Kyungjune Baek, Duhyeon Bang, and Hyunjung Shim. Gridmix: Strong regularization through local context mapping. *Pattern Recognition*, 2021.
- [5] Hedi Ben-Younes, Rémi Cadene, Matthieu Cord, and Nicolas Thome. Mutan: Multimodal tucker fusion for visual question answering. In *Proceedings of the IEEE interna*tional conference on computer vision, pages 2612–2620, 2017.
- [6] David Berthelot, Nicholas Carlini, Ekin D. Cubuk, Alex Kurakin, Kihyuk Sohn, Han Zhang, and Colin Raffel. Remixmatch: Semi-supervised learning with distribution alignment and augmentation anchoring. In *International Conference on Learning Representations*, 2020.
- [7] David Berthelot, Nicholas Carlini, Ian Goodfellow, Nicolas Papernot, Avital Oliver, and Colin Raffel. Mixmatch: a holistic approach to semi-supervised learning. *NeurIPS*, 2019.
- [8] Shahine Bouabid and Vincent Delaitre. Mixup regularization for region proposal based object detectors. arXiv preprint arXiv:2003.02065, 2020.
- [9] Leo Breiman. Bagging predictors. *Machine learning*, 24(2):123–140, 1996.
- [10] Cristian Bucilua, Rich Caruana, and Alexandru Niculescu-Mizil. Model compression. In *Proceedings of the 12th ACM SIGKDD international conference on Knowledge discovery and data mining*, pages 535–541, 2006.
- [11] Remi Cadene, Hedi Ben-Younes, Matthieu Cord, and Nicolas Thome. Murel: Multimodal relational reasoning for visual question answering. In *Proceedings of the IEEE Con*ference on Computer Vision and Pattern Recognition, pages 1989–1998, 2019.
- [12] Luigi Carratino, Moustapha Cisse, Rodolphe Jenatton, and Jean-Philippe Vert. On mixup regularization. Technical report, arXiv, 2020. 2006.06049.
- [13] Rich Caruana. Multitask learning. *Machine learning*, 28(1):41–75, 1997.

- [14] Defang Chen, Jian-Ping Mei, Can Wang, Yan Feng, and Chun Chen. Online knowledge distillation with diverse peers. In *AAAI*, pages 3430–3437, 2020.
- [15] Nadezhda Chirkova, Ekaterina Lobacheva, and Dmitry Vetrov. Deep ensembles on a fixed memory budget: One wide network or several thinner ones? *arXiv preprint arXiv:2005.07292*, 2020.
- [16] Patryk Chrabaszcz, Ilya Loshchilov, and Frank Hutter. A downsampled variant of imagenet as an alternative to the cifar datasets. arXiv preprint arXiv:1707.08819, 2017.
- [17] Ali Dabouei, Sobhan Soleymani, Fariborz Taherkhani, and Nasser M Nasrabadi. Supermix: Supervising the mixing data augmentation. *arXiv preprint arXiv:2003.05034*, 2020.
- [18] J. Deng, W. Dong, R. Socher, L.-J. Li, K. Li, and L. Fei-Fei. ImageNet: A Large-Scale Hierarchical Image Database. In CVPR09, 2009.
- [19] Terrance DeVries and Graham W Taylor. Improved regularization of convolutional neural networks with cutout. arXiv preprint arXiv:1708.04552, 2017.
- [20] Thomas G Dietterich. Ensemble methods in machine learning. In *International workshop on multiple classifier systems*, pages 1–15. Springer, 2000.
- [21] Nikita Durasov, Timur Bagautdinov, Pierre Baque, and Pascal Fua. Masksembles for uncertainty estimation. arXiv preprint arXiv:2012.08334, 2020.
- [22] Michael Dusenberry, Ghassen Jerfel, Yeming Wen, Yian Ma, Jasper Snoek, Katherine Heller, Balaji Lakshminarayanan, and Dustin Tran. Efficient and scalable bayesian neural nets with rank-1 factors. In *International conference on machine learning*, pages 2782–2792. PMLR, 2020.
- [23] Mojtaba Faramarzi, Mohammad Amini, Akilesh Badrinaaraayanan, Vikas Verma, and Sarath Chandar. Patchup: A regularization technique for convolutional neural networks, 2020.
- [24] Stanislav Fort, Huiyi Hu, and Balaji Lakshminarayanan. Deep ensembles: A loss landscape perspective. arXiv preprint arXiv:1912.02757, 2019.
- [25] Jonathan Frankle and Michael Carbin. The lottery ticket hypothesis: Finding sparse, trainable neural networks. In 7th International Conference on Learning Representations, ICLR 2019, New Orleans, LA, USA, May 6-9, 2019. Open-Review.net, 2019.
- [26] Geoff French, Timo Aila, Samuli Laine, Michal Mackiewicz, and Graham Finlayson. Semi-supervised semantic segmentation needs strong, high-dimensional perturbations. arXiv preprint arXiv:1906.01916, 2019.
- [27] Geoff French, Avital Oliver, and Tim Salimans. Milking cowmask for semi-supervised image classification. arXiv preprint arXiv:2003.12022, 2020.
- [28] Yarin Gal and Zoubin Ghahramani. Dropout as a bayesian approximation: Representing model uncertainty in deep learning. In *international conference on machine learning*, pages 1050–1059, 2016.
- [29] Yuan Gao, Zixiang Cai, and Lei Yu. Intra-ensemble in neural networks. arXiv preprint arXiv:1904.04466, 2019.

- [30] Timur Garipov, Pavel Izmailov, Dmitrii Podoprikhin, Dmitry P Vetrov, and Andrew G Wilson. Loss surfaces, mode connectivity, and fast ensembling of dnns. In Advances in Neural Information Processing Systems, pages 8789–8798, 2018.
- [31] Golnaz Ghiasi, Tsung-Yi Lin, and Quoc V Le. Dropblock: A regularization method for convolutional networks. In Advances in neural information processing systems, pages 10727–10737, 2018.
- [32] Raphael Gontijo-Lopes, Sylvia J Smullin, Ekin D Cubuk, and Ethan Dyer. Affinity and diversity: Quantifying mechanisms of data augmentation. *arXiv preprint arXiv:2002.08973*, 2020.
- [33] Chuan Guo, Geoff Pleiss, Yu Sun, and Kilian Q Weinberger. On calibration of modern neural networks. arXiv preprint arXiv:1706.04599, 2017.
- [34] Hongyu Guo, Yongyi Mao, and Richong Zhang. Mixup as locally linear out-of-manifold regularization. In *Proceed-ings of the AAAI Conference on Artificial Intelligence*, volume 33, pages 3714–3722, 2019.
- [35] Fredrik K Gustafsson, Martin Danelljan, and Thomas B Schon. Evaluating scalable bayesian deep learning methods for robust computer vision. In *Proceedings of the IEEE/CVF Conference on Computer Vision and Pattern Recognition Workshops*, pages 318–319, 2020.
- [36] Lars Kai Hansen and Peter Salamon. Neural network ensembles. *IEEE transactions on pattern analysis and ma*chine intelligence, 12(10):993–1001, 1990.
- [37] Ethan Harris, Antonia Marcu, Matthew Painter, Mahesan Niranjan, Adam Prügel-Bennett, and Jonathon Hare. Fmix: Enhancing mixed sample data augmentation. *arXiv preprint arXiv:2002.12047*, 2020.
- [38] Marton Havasi, Rodolphe Jenatton, Stanislav Fort, Jeremiah Liu, Jasper Roland Snoek, Balaji Lakshminarayanan, Andrew Mingbo Dai, and Dustin Tran. Training independent subnetworks for robust prediction. In *International Conference on Learning Representations*, 2021.
- [39] Bobby He, Balaji Lakshminarayanan, and Yee Whye Teh. Bayesian deep ensembles via the neural tangent kernel. *arXiv preprint arXiv:2007.05864*, 2020.
- [40] Kaiming He, Xiangyu Zhang, Shaoqing Ren, and Jian Sun. Deep residual learning for image recognition. In *Proceedings of the IEEE conference on computer vision and pattern recognition*, pages 770–778, 2016.
- [41] Kaiming He, Xiangyu Zhang, Shaoqing Ren, and Jian Sun. Identity mappings in deep residual networks. In *ECCV* (4), pages 630–645, 2016.
- [42] Zhuoxun He, Lingxi Xie, Xin Chen, Ya Zhang, Yanfeng Wang, and Qi Tian. Data augmentation revisited: Rethinking the distribution gap between clean and augmented data. *CoRR*, 2019.
- [43] Dan Hendrycks and Thomas Dietterich. Benchmarking neural network robustness to common corruptions and perturbations. In *International Conference on Learning Rep*resentations, 2019.
- [44] Dan Hendrycks, Norman Mu, Ekin Dogus Cubuk, Barret Zoph, Justin Gilmer, and Balaji Lakshminarayanan. Aug-

- mix: A simple data processing method to improve robustness and uncertainty. In *International Conference on Learn*ing Representations, 2019.
- [45] Geoffrey Hinton, Oriol Vinyals, and Jeff Dean. Distilling the knowledge in a neural network. *stat*, 1050:9, 2015.
- [46] Elad Hoffer, Tal Ben-Nun, Itay Hubara, Niv Giladi, Torsten Hoefler, and Daniel Soudry. Augment your batch: Improving generalization through instance repetition. In *Proceed*ings of the IEEE/CVF Conference on Computer Vision and Pattern Recognition (CVPR), June 2020.
- [47] Gao Huang, Yixuan Li, Geoff Pleiss, Zhuang Liu, John E. Hopcroft, and Kilian Q. Weinberger. Snapshot ensembles: Train 1, get m for free. 2017.
- [48] Hiroshi Inoue. Data augmentation by pairing samples for images classification. CoRR, 2018.
- [49] Pavel Izmailov, Dmitrii Podoprikhin, Timur Garipov, Dmitry Vetrov, and Andrew Gordon Wilson. Averaging weights leads to wider optima and better generalization. In Ricardo Silva, Amir Globerson, and Amir Globerson, editors, 34th Conference on Uncertainty in Artificial Intelligence 2018, UAI 2018, 34th Conference on Uncertainty in Artificial Intelligence 2018, UAI 2018, pages 876–885. Association For Uncertainty in Artificial Intelligence (AUAI), 2018. 34th Conference on Uncertainty in Artificial Intelligence 2018, UAI 2018; Conference date: 06-08-2018 Through 10-08-2018.
- [50] Alex Kendall, Yarin Gal, and Roberto Cipolla. Multi-task learning using uncertainty to weigh losses for scene geometry and semantics. In *Proceedings of the IEEE conference* on computer vision and pattern recognition, pages 7482– 7491, 2018.
- [51] JangHyun Kim, Wonho Choo, Hosan Jeong, and Hyun Oh Song. Co-mixup: Saliency guided joint mixup with supermodular diversity. In *International Conference on Learning Representations*, 2021.
- [52] Jiyeon Kim, Ik-Hee Shin, Jong-Ryul Lee, and Yong-Ju Lee. Where to cut and paste: Data regularization with selective features. In 2020 International Conference on Information and Communication Technology Convergence (ICTC), pages 1219–1221. IEEE, 2020.
- [53] Jang-Hyun Kim, Wonho Choo, and Hyun Oh Song. Puzzle mix: Exploiting saliency and local statistics for optimal mixup. In *International Conference on Machine Learning*, pages 5275–5285. PMLR, 2020.
- [54] Alex Krizhevsky et al. Learning multiple layers of features from tiny images. 2009.
- [55] Anders Krogh and Jesper Vedelsby. Neural network ensembles, cross validation, and active learning. In *Advances* in neural information processing systems, pages 231–238, 1995.
- [56] Balaji Lakshminarayanan, Alexander Pritzel, and Charles Blundell. Simple and scalable predictive uncertainty estimation using deep ensembles. In *Advances in neural infor*mation processing systems, pages 6402–6413, 2017.
- [57] Xu Lan, Xiatian Zhu, and Shaogang Gong. Knowledge distillation by on-the-fly native ensemble. In *Proceedings of the 32nd International Conference on Neural Information Processing Systems*, pages 7528–7538, 2018.

- [58] Yann Lecun, J. S. Denker, Sara A. Solla, R. E. Howard, and L.D. Jackel. Optimal brain damage. In David Touretzky, editor, Advances in Neural Information Processing Systems (NIPS 1989), Denver, CO, volume 2. Morgan Kaufmann, 1990.
- [59] Jin-Ha Lee, Muhammad Zaigham Zaheer, Marcella Astrid, and Seung-Ik Lee. Smoothmix: A simple yet effective data augmentation to train robust classifiers. In *Proceedings of* the IEEE/CVF Conference on Computer Vision and Pattern Recognition Workshops, pages 756–757, 2020.
- [60] Kibok Lee, Yian Zhu, Kihyuk Sohn, Chun-Liang Li, Jin-woo Shin, and Honglak Lee. i-mix: A strategy for regular-izing contrastive representation learning. In *International Conference on Learning Representations*, 2021.
- [61] Stefan Lee, Senthil Purushwalkam, Michael Cogswell, David J. Crandall, and Dhruv Batra. Why M heads are better than one: Training a diverse ensemble of deep networks. CoRR, 2015.
- [62] Boyi Li, Felix Wu, Ser-Nam Lim, Serge Belongie, and Kilian Q. Weinberger. On feature normalization and data augmentation. arXiv preprint arXiv:2002.11102, 2020.
- [63] Hao Li, Asim Kadav, Igor Durdanovic, Hanan Samet, and Hans Peter Graf. Pruning filters for efficient convnets. In *International Conference on Learning Representations*, 2017.
- [64] Daojun Liang, Feng Yang, Tian Zhang, and Peter Yang. Understanding mixup training methods. *IEEE Access*, 6:58774–58783, 2018.
- [65] Tsung-Yi Lin, Priya Goyal, Ross Girshick, Kaiming He, and Piotr Dollár. Focal loss for dense object detection. In Proceedings of the IEEE international conference on computer vision, pages 2980–2988, 2017.
- [66] Jakob Lindqvist, Amanda Olmin, Fredrik Lindsten, and Lennart Svensson. A general framework for ensemble distribution distillation. arXiv preprint arXiv:2002.11531, 2020
- [67] Ekaterina Lobacheva, Nadezhda Chirkova, Maxim Kodryan, and Dmitry P Vetrov. On power laws in deep ensembles. In H. Larochelle, M. Ranzato, R. Hadsell, M. F. Balcan, and H. Lin, editors, *Advances in Neural Informa*tion Processing Systems, volume 33, pages 2375–2385. Curran Associates, Inc., 2020.
- [68] Wesley J Maddox, Pavel Izmailov, Timur Garipov, Dmitry P Vetrov, and Andrew Gordon Wilson. A simple baseline for bayesian uncertainty in deep learning. In Advances in Neural Information Processing Systems, pages 13153–13164, 2019.
- [69] Eran Malach, Gilad Yehudai, Shai Shalev-Schwartz, and Ohad Shamir. Proving the lottery ticket hypothesis: Pruning is all you need. In *International Conference on Machine Learning*, pages 6682–6691. PMLR, 2020.
- [70] Pavlo Molchanov, Stephen Tyree, Tero Karras, Timo Aila, and Jan Kautz. Pruning convolutional neural networks for resource efficient transfer learning. arXiv preprint arXiv:1611.06440, 3, 2016.
- [71] Brady Neal, Sarthak Mittal, Aristide Baratin, Vinayak Tantia, Matthew Scicluna, Simon Lacoste-Julien, and Ioannis Mitliagkas. A modern take on the bias-variance tradeoff in neural networks. arXiv preprint arXiv:1810.08591, 2018.

- [72] Nils J. Nilsson. Learning machines: Foundations of trainable pattern-classifying systems. 1965.
- [73] Viktor Olsson, Wilhelm Tranheden, Juliano Pinto, and Lennart Svensson. Classmix: Segmentation-based data augmentation for semi-supervised learning. In Proceedings of the IEEE/CVF Winter Conference on Applications of Computer Vision (WACV), pages 1369–1378, January 2021.
- [74] David Opitz and Richard Maclin. Popular ensemble methods: An empirical study. *Journal of artificial intelligence* research, 11:169–198, 1999.
- [75] Ian Osband, Charles Blundell, Alexander Pritzel, and Benjamin Van Roy. Deep exploration via bootstrapped dqn. arXiv preprint arXiv:1602.04621, 2016.
- [76] Yaniv Ovadia, Emily Fertig, Jie Ren, Zachary Nado, David Sculley, Sebastian Nowozin, Joshua Dillon, Balaji Lakshminarayanan, and Jasper Snoek. Can you trust your model's uncertainty? evaluating predictive uncertainty under dataset shift. In *Advances in Neural Information Processing Sys*tems, pages 13991–14002, 2019.
- [77] Tianyu Pang, Kun Xu, Chao Du, Ning Chen, and Jun Zhu. Improving adversarial robustness via promoting ensemble diversity. In *International Conference on Machine Learn*ing, pages 4970–4979, 2019.
- [78] Adam Paszke, Sam Gross, Soumith Chintala, Gregory Chanan, Edward Yang, Zachary DeVito, Zeming Lin, Alban Desmaison, Luca Antiga, and Adam Lerer. Automatic differentiation in pytorch. 2017.
- [79] Ankit Pensia, Shashank Rajput, Alliot Nagle, Harit Vishwakarma, and Dimitris Papailiopoulos. Optimal lottery tickets via subsetsum: Logarithmic over-parameterization is sufficient. arXiv preprint arXiv:2006.07990, 2020.
- [80] Michael P Perrone and Leon N Cooper. When networks disagree: Ensemble methods for hybrid neural networks. Technical report, BROWN UNIV PROVIDENCE RI INST FOR BRAIN AND NEURAL SYSTEMS, 1992.
- [81] Jie Qin, Jiemin Fang, Qian Zhang, Wenyu Liu, Xingang Wang, and Xinggang Wang. Resizemix: Mixing data with preserved object information and true labels. *arXiv* preprint *arXiv*:2012.11101, 2020.
- [82] Alexandre Rame and Matthieu Cord. Dice: Diversity in deep ensembles via conditional redundancy adversarial estimation. In *International Conference on Learning Representations*, 2021.
- [83] Hippolyt Ritter, Aleksandar Botev, and David Barber. A scalable laplace approximation for neural networks. In 6th International Conference on Learning Representations, ICLR 2018-Conference Track Proceedings, volume 6. International Conference on Representation Learning, 2018.
- [84] Lior Rokach. Ensemble-based classifiers. Artificial intelligence review, 33(1-2):1–39, 2010.
- [85] Ramprasaath R Selvaraju, Michael Cogswell, Abhishek Das, Ramakrishna Vedantam, Devi Parikh, and Dhruv Batra. Grad-cam: Visual explanations from deep networks via gradient-based localization. In *Proceedings of the IEEE in*ternational conference on computer vision, pages 618–626, 2017.

- [86] Ozan Sener and Vladlen Koltun. Multi-task learning as multi-objective optimization. arXiv preprint arXiv:1810.04650, 2018.
- [87] Tom Sercu, Christian Puhrsch, Brian Kingsbury, and Yann LeCun. Very deep multilingual convolutional neural networks for lvcsr. In 2016 IEEE International Conference on Acoustics, Speech and Signal Processing (ICASSP), pages 4955–4959. IEEE, 2016.
- [88] Patrice Simard, Yann LeCun, and John S Denker. Efficient pattern recognition using a new transformation distance. In Advances in neural information processing systems, pages 50–58, 1993.
- [89] Masoumeh Soflaei, Hongyu Guo, Ali Al-Bashabsheh, Yongyi Mao, and Richong Zhang. Aggregated learning: A vector-quantization approach to learning neural network classifiers. In *Proceedings of the AAAI Conference on Arti*ficial Intelligence, volume 34, pages 5810–5817, 2020.
- [90] Guocong Song and Wei Chai. Collaborative learning for deep neural networks. In *Advances in Neural Information Processing Systems*, pages 1832–1841, 2018.
- [91] Nitish Srivastava, Geoffrey Hinton, Alex Krizhevsky, Ilya Sutskever, and Ruslan Salakhutdinov. Dropout: a simple way to prevent neural networks from overfitting. *The jour*nal of machine learning research, 15(1):1929–1958, 2014.
- [92] Cecilia Summers and Michael J Dinneen. Improved mixedexample data augmentation. In Applications of Computer Vision (WACV), 2019 IEEE Winter Conference on. IEEE, 2019.
- [93] Mihai Suteu and Yike Guo. Regularizing deep multitask networks using orthogonal gradients. arXiv preprint arXiv:1912.06844, 2019.
- [94] Christian Szegedy, Wei Liu, Yangqing Jia, Pierre Sermanet, Scott Reed, Dragomir Anguelov, Dumitru Erhan, Vincent Vanhoucke, and Andrew Rabinovich. Going deeper with convolutions. In *Proceedings of the IEEE conference on computer vision and pattern recognition*, pages 1–9, 2015.
- [95] Ryo Takahashi, Takashi Matsubara, and Kuniaki Uehara. Data augmentation using random image cropping and patching for deep cnns. *IEEE Transactions on Circuits and Systems for Video Technology*, 2019.
- [96] Naftali Tishby. The information bottleneck method. In Proc. 37th Annual Allerton Conference on Communications, Control and Computing, 1999, pages 368–377, 1999.
- [97] Yuji Tokozume, Yoshitaka Ushiku, and Tatsuya Harada. Between-class learning for image classification. In *Proceedings of the IEEE Conference on Computer Vision and Pattern Recognition (CVPR)*, June 2018.
- [98] Yuji Tokozume, Yoshitaka Ushiku, and Tatsuya Harada. Learning from between-class examples for deep sound recognition. In *International Conference on Learning Rep*resentations, 2018.
- [99] Linh Tran, Bastiaan S. Veeling, Kevin Roth, Jakub Swiatkowski, Joshua V. Dillon, Jasper Snoek, Stephan Mandt, Tim Salimans, Sebastian Nowozin, and Rodolphe Jenatton. Hydra: Preserving ensemble diversity for model distillation. arXiv preprint arXiv:2001.04694, 2020.
- [100] A. F. M. Shahab Uddin, Mst. Sirazam Monira, Wheemyung Shin, TaeChoong Chung, and Sung-Ho Bae. Saliencymix:

- A saliency guided data augmentation strategy for better regularization, 2020.
- [101] Vikas Verma, Alex Lamb, Christopher Beckham, Amir Najafi, Ioannis Mitliagkas, David Lopez-Paz, and Yoshua Bengio. Manifold mixup: Better representations by interpolating hidden states. In Kamalika Chaudhuri and Ruslan Salakhutdinov, editors, Proceedings of the 36th International Conference on Machine Learning, volume 97 of Proceedings of Machine Learning Research, pages 6438–6447, Long Beach, California, USA, 09–15 Jun 2019. PMLR.
- [102] Devesh Walawalkar, Zhiqiang Shen, Zechun Liu, and Marios Savvides. Attentive cutmix: An enhanced data augmentation approach for deep learning based image classification. In ICASSP 2020-2020 IEEE International Conference on Acoustics, Speech and Signal Processing (ICASSP), pages 3642–3646. IEEE, 2020.
- [103] Xiaofang Wang, Dan Kondratyuk, Kris M. Kitani, Yair Movshovitz-Attias, and Elad Eban. Multiple networks are more efficient than one: Fast and accurate models via ensembles and cascades. arXiv preprint arXiv:2012.01988, 2020.
- [104] Abdul Wasay, Brian Hentschel, Yuze Liao, Sanyuan Chen, and Stratos Idreos. Mothernets: Rapid deep ensemble learning. In I. Dhillon, D. Papailiopoulos, and V. Sze, editors, *Proceedings of Machine Learning and Systems*, volume 2, pages 199–215, 2020.
- [105] Yeming Wen, Ghassen Jerfel, Rafael Muller, Michael W Dusenberry, Jasper Snoek, Balaji Lakshminarayanan, and Dustin Tran. Combining ensembles and data augmentation can harm your calibration. In *International Conference on Learning Representations*, 2021.
- [106] Florian Wenzel, Jasper Snoek, Dustin Tran, and Rodolphe Jenatton. Hyperparameter ensembles for robustness and uncertainty quantification. arXiv preprint arXiv:2006.13570, 2020.
- [107] Florian Wenzel, Jasper Snoek, Dustin Tran, and Rodolphe Jenatton. Hyperparameter ensembles for robustness and uncertainty quantification. arXiv preprint arXiv:2006.13570, 2020.
- [108] Andrew Gordon Wilson. The case for bayesian deep learning. CoRR, abs/2001.10995, 2020.
- [109] Andrew Gordon Wilson and Pavel Izmailov. Bayesian deep learning and a probabilistic perspective of generalization. arXiv preprint arXiv:2002.08791, 2020.
- [110] David H Wolpert. Stacked generalization. *Neural networks*, 5(2):241–259, 1992.
- [111] A Wu, S Nowozin, E Meeds, RE Turner, JM Hernández-Lobato, and AL Gaunt. Deterministic variational inference for robust bayesian neural networks. In 7th International Conference on Learning Representations, ICLR 2019, 2019.
- [112] Yoichi Yaguchi, Fumiyuki Shiratani, and Hidekazu Iwaki. Mixfeat: Mix feature in latent space learns discriminative space, 2019.
- [113] Taojiannan Yang, Sijie Zhu, and Chen Chen. Gradaug: A new regularization method for deep neural networks. Advances in Neural Information Processing Systems, 33, 2020.

- [114] Sangdoo Yun, Dongyoon Han, Seong Joon Oh, Sanghyuk Chun, Junsuk Choe, and Youngjoon Yoo. Cutmix: Regularization strategy to train strong classifiers with localizable features. In *Proceedings of the IEEE International Conference on Computer Vision*, pages 6023–6032, 2019.
- [115] Sergey Zagoruyko and Nikos Komodakis. Wide residual networks. In Edwin R. Hancock Richard C. Wilson and William A. P. Smith, editors, *Proceedings of the British Machine Vision Conference (BMVC)*, pages 87.1–87.12. BMVA Press, September 2016.
- [116] Chiyuan Zhang, Samy Bengio, Moritz Hardt, Benjamin Recht, and Oriol Vinyals. Understanding deep learning requires rethinking generalization. 2017.
- [117] Hongyi Zhang, Moustapha Cisse, Yann N Dauphin, and David Lopez-Paz. mixup: Beyond empirical risk minimization. In *International Conference on Learning Representations*, 2018.
- [118] Linjun Zhang, Zhun Deng, Kenji Kawaguchi, Amirata Ghorbani, and James Zou. How does mixup help with robustness and generalization? *arXiv preprint arXiv:2010.04819*, 2020.
- [119] Ruqi Zhang, Chunyuan Li, Jianyi Zhang, Changyou Chen, and Andrew Gordon Wilson. Cyclical stochastic gradient mcmc for bayesian deep learning. In *International Conference on Learning Representations*, 2019.
- [120] Shuai Zhao, Liguang Zhou, Wenxiao Wang, Deng Cai, Tin Lun Lam, and Yangsheng Xu. Splitnet: Divide and co-training. *arXiv preprint arXiv:2011.14660*, 2020.
- [121] Michael Zhu and Suyog Gupta. To prune, or not to prune: exploring the efficacy of pruning for model compression. *arXiv* preprint arXiv:1710.01878, 2017.

6. Appendix

The sections in this Appendix follow the same order than their related sections in the main paper. We first illustrate the reweighting of the loss components in Appendix 6.1. Appendix 6.2 elaborates on our analysis of filters activity. Appendix 6.3 clarifies our framework generalization with M > 2 subnetworks. We then describe in greater details our experimental setting in Appendix 6.4. Appendix 6.5 showcases training dynamics. We provide a quick refresher on common MSDA techniques in Appendix 6.6. Appendix 6.7 studies the importance of α . Appendix 6.8 analyzes ensembles of Cut-MixMo with CutMix that reach state of the art. Finally, we provide a pseudo-code in Algorithm 1.

6.1. Weighting function w_r

As outlined in Section 3.3, the asymmetry in the mixing mechanism leads to asymmetry in the relative importance of the two inputs. Thus we reweight the loss components with function w_r , defined as $w_r(\kappa) = 2 \frac{\kappa^{1/r}}{\kappa^{1/r} + (1-\kappa)^{1/r}}$. It rescales the mixing ratio κ through the use of a $\frac{1}{r}$ root operator. In the main paper, we have focused on r = 3.

Fig. 11 illustrates how w_r behaves for $r \in \{1, 2, 3, 4, 10\}$ and $r \to \infty$. The first extreme r = 1 matches the diagonal $w_r(\kappa) = 2\kappa$, without rescaling of κ , similarly to what is customary in MSDA. Our experiments in Section 4.3.3 justified the initial idea to shift the weighting function closer to the horizontal and constant curve $w_r(\kappa) = 1$ with higher r. In the other experiments, we always set r=3.

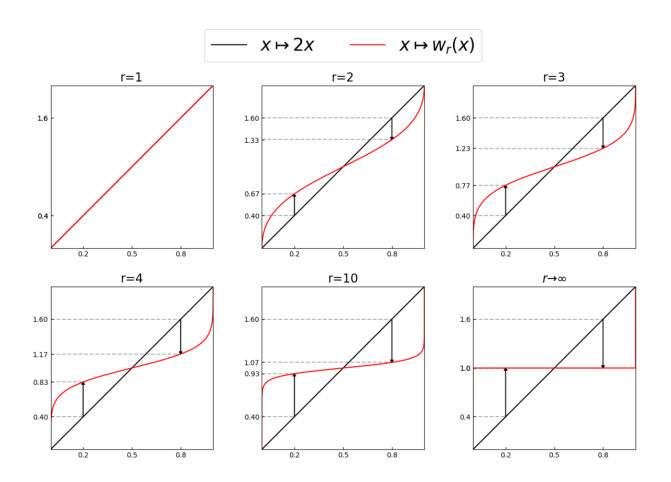


Figure 11: Curves of the reweighting operation that projects κ to the flattened ratio $w_r(\kappa)$

6.2. Filters activity

We argued in Section 3.4 that MixMo better leverages additional parameters in wider networks. Concretely, a larger proportion of filters in large networks really help for

Table 7: **Proportion** (%) of active filters in core network vs. width w for a WRN-28-w on CIFAR 100 and different activity thresholds t_a .

Method	Width	$t_a = 0.2$	$t_a = 0.3$	$t_a = 0.4$	$t_a = 0.5$
	2	98.9	98.8	97.8	93.3
	3	97.3	96.4	93.2	87.5
	4	96.5	95.2	91.2	81.6
Vanilla	5	95.1	91.7	85.7	73.3
	7	92.6	88.2	81.0	69.5
	10	87.8	80.4	71.5	57.3
	14	83.9	74.0	61.6	46.8
	2	99.2	99.0	97.8	95.3
	3	98.7	98.5	97.2	93.4
	4	98.1	97.4	94.0	87.3
CutMix	5	97.0	96.1	90.7	80.6
	7	95.8	94.0	86.2	74.6
	2 98.9 98.8 97.8 3 97.3 96.4 93.2 4 96.5 95.2 91.2 91.2 92.6 88.2 81.0 10 87.8 80.4 71.5 14 83.9 74.0 61.6	67.0			
	14	89.4	81.9	70.3	50.9
	2	100.0	100.0	99.4	97.3
	3	99.8	99.8	99.7	98.7
	4	99.7	99.7	99.6	98.7
Vanilla 3 97.3 96.4 4 96.5 95.2 Vanilla 5 95.1 91.7 7 92.6 88.2 10 87.8 80.4 14 83.9 74.0 2 99.2 99.0 3 98.7 98.5 4 98.1 97.4 CutMix 5 97.0 96.1 7 95.8 94.0 10 93.5 88.4 14 89.4 81.9 Cut-MixMo 2 100.0 100.0 3 99.8 99.8 4 99.7 99.7 Cut-MixMo 5 99.3 99.3 7 98.9 98.8 10 98.5 98.2	99.3	98.9	97.4		
	7	98.9	98.8	98.0	95.2
	10	98.5	98.2	96.8	92.4
	14	97.5	96.3	93.1	82.6

classification as demonstrated in Fig. 4a and 4b in the main paper. Following common practices in the structured pruning literature [63], we used the l_1 -norm of convolutional filters as a proxy for importance. These 3D filters are of shape $n_i \times k \times k$ with n_i the number of input channels and k the kernel size. In Fig. 4b, we arbitrarily defined a filter as active if its l_1 -norm is at least 40% of the highest filter l_1 -norm in that filter's layer. We report the average percentage of active filters across all filters in the core network C, for 3 learning strategies: vanilla, CutMix and Cut-MixMo.

The threshold $t_a = 0.4$ was chosen for visualization purposes. Nevertheless, the observed trend in activity proportions remains for varying thresholds in Tab. 7. For example, for the lax $t_a=0.2$, CutMix uses 93.5% of filters vs. 98.5%for Cut-MixMo.

6.3. Generalization to M > 2 heads

We have mostly discussed our MixMo framework with M = 2 subnetworks. For better readability, we referred to the mixing ratios κ and $1 - \kappa$ with $\kappa \sim$ Beta (α, α) . It's equivalent to a more generic formulation $(\kappa_0, \kappa_1) \in \text{Dir}_2(\alpha)$ from a symmetric Dirichlet distribution with concentration parameter α . This leads to the alternate equations $\mathcal{L}_{\text{MixMo}} = \sum_{i=0,1} w_r(\kappa_i) \mathcal{L}_{\text{CE}}(y_i, \hat{y}_i),$

where
$$w_r(\kappa_i) = 2 \frac{\kappa_i^{\gamma \gamma}}{\sum_{j=0,1} \kappa_j^{1/r}}$$

where $w_r(\kappa_i) = 2\frac{\kappa_i^{1/r}}{\sum_{j=0,1} \kappa_j^{1/r}}$. Now generalization to the general case $M \geq 2$ is straightforward. We draw a tuple $\{\kappa_i\}_{0 \le i \le M} \sim \text{Dir}_M(\alpha)$ and optimize the training loss:

$$\mathcal{L}_{\text{MixMo}} = \sum_{i=0}^{M-1} w_r(\kappa_i) \mathcal{L}_{CE}(y_i, \hat{y}_i), \qquad (4)$$

where the new weighting naturally follows:

$$w_r(\kappa_i) = M \frac{\kappa_i^{1/r}}{\sum_{j=0}^{M-1} \kappa_j^{1/r}}, \forall i \in \{0, \dots, M-1\}.$$
 (5)

The remaining point is the generalization of the mixing block \mathcal{M} , that relies on the existence of MSDA methods for M>2 inputs. The linear interpolation can be easily expanded as in Mixup:

$$\mathcal{M}_{\text{Linear-MixMo}}\left(\{l_i\}\right) = M \sum_{i=0}^{M-1} \kappa_i l_i, \tag{6}$$

where $l_i=c_i(x_i)$. However, extensions for other masking MSDA have only recently started to emerge [51]. For example, CutMix is not trivially generalizable to M>2, as the patches could overlap and hide important semantic components. In our experiments, a soft extension of Cut-MixMo performs best: it first linearly interpolates M-1 inputs and then patches a region from the M-th:

$$\mathcal{M}_{\text{Cut-MixMo}}(\{l_i\}) = M[\mathbb{1}_{\mathcal{M}} \odot l_k + (\mathbb{1} - \mathbb{1}_{\mathcal{M}}) \odot \sum_{i=0, i \neq k}^{M-1} \frac{\kappa_i}{1 - \kappa_k} l_i],$$
(7)

where $\mathbb{1}_{\mathcal{M}}$ is a rectangle of area ratio κ_k and k sampled uniformly in $\{0, 1, \ldots, M-1\}$. However, it has been less successful than M=2, as only two subnetworks can fit independently in standard parameterization regimes. Future work could design new framework components, such as specific mixing blocks, to tackle these limits.

6.4. Experimental details

We first used the popular image classification **datasets** CIFAR-100 and CIFAR-10 [54]. They contain $60k\ 32\times 32$ natural and colored images in respectively 100 classes and 10 classes, with 50k training images and 10k test images. At a larger scale, we study Tiny ImageNet [16], a down-sampled version of ImageNet [18]. It contains 200 different categories, $100k\ 64\times 64$ training images (*i.e.* 500 images per class) and 10k test images.

Our code was adapted from the official MIMO [38] implementation¹. For CIFAR, we used standard architecture WRN-28-w, with a focus on w=10. We re-use the **hyper-parameters** configuration from MIMO [38]. The optimizer is SGD with learning rate of $\frac{0.1}{b} \times \frac{\text{batch-size}}{128}$, batch size 64, linear warmup over 1 epoch, decay rate 0.1 at steps $\{75, 150, 225\}$, l_2 regularization 3e-4. We follow standard MSDA practices [3, 53, 114] and set the maximum number of epochs to 300. For Tiny ImageNet, we use PreActResNet-18-w, with $w \in \{1, 2, 3\}$ times more filters. We re-use the hyper-parameters from Puzzle-Mix [53].

Table 8: WRN-28-10 on CIFAR without early stopping.

Dataset		C	CIFAR-10	CIFAR-10		
Approach	Time Tr./Inf.	Top1 %	Top5	$\begin{array}{c} \mathrm{NLL}_c \\ 10^{-2} \end{array}$	Top1 %	$\begin{array}{c} \mathrm{NLL}_c \\ 10^{-2} \end{array}$
Vanilla	1/1	81.47	95.57	73.6	96.31	12.5
Mixup		83.15	95.75	66.3	97.00	11.3
CutMix		83.74	96.18	65.4	97.21	9.7
CowMix		83.00	95.95	67.3	97.24	9.7
Puzzle-Mix†	2/1	84.05	96.08	66.9	-	-
GradAug [†] + CutMix [†]	3/1	83.98 85.25	96.28 96.85	-	-	-
DE (2 Nets)	2/2	83.15	96.30	66.0	96.58	11.1
+ CutMix		85.46	96.90	57.4	97.51	8.7
MIMO		82.04	95.75	69.1	96.33	12.1
Linear-MixMo	2/1	81.88	95.97	67.8	96.55	11.4
+ CutMix		84.55	96.95	57.4	97.34	8.9
Cut-MixMo		84.07	96.97	56.6	97.26	8.7
+ CutMix		85.17	97.28	54.4	97.33	8.5
MIMO		82.74	95.90	67.0	96.66	11.5
Linear-MixMo	4/1	82.53	96.08	65.8	96.78	10.8
+ CutMix		85.24	96.97	56.3	97.53	8.8
Cut-MixMo		85.32	97.12	53.6	97.42	8.1
+ CutMix		85.59	97.33	53.2	97.70	8.0

The optimizer is SGD with learning rate of $\frac{0.2}{b}$, batch size 100, decay rate 0.1 at steps $\{600, 900\}$, 1200 epochs maximum, weight decay 1e-4. Our experiments ran on a single NVIDIA 12Go-TITAN X Pascal GPU. We will soon release our code and pre-trained models to facilitate reproducibility.

Batch repetition increases performances at the cost of **longer training**, which may be discouraging for some practitioners. Thus in addition to b=4 as in MIMO [38], we often consider the quicker b=2. Note that most of our concurrent approaches also increase training time: DE [56] via several independent trainings, Puzzle-Mix [53] via saliency detection ($\approx \times 2$), GradAug [113] via multiple subnetworks predictions ($\approx \times 3$) or Mixup BA [46] via 10 batch augmentations ($\approx \times 8$ with our hardware on a single GPU).

We reproduce the **experimental setting** from seminal CutMix [114], Manifold Mixup [101] and other works such as the recent state-of-the-art ResizeMix [81]: in absence of a validation dataset, results are reported at the epoch that yields the best test accuracy. For fair comparison, we apply this setting for all concurrent approaches. For the sake of completeness, Table 8 presents the results without early stopping on the main experiment (CIFAR with a standard WRN-28-10). We recover the exact same ranking among methods, tendencies and conclusions as Table 1.

MixMo operates in the features space and is complementary with **pixels augmentations**, *i.e.* cropping, Aug-Mix. The standard vanilla pixels data augmentation [40] consists of 4 pixels padding, random cropping and horizontal flipping. When combined with CutMix, notably to benefit from multilabel smoothing, the input may be of the form: $(m_x(x_i, x_k, \lambda), x_j)$, where x_k is randomly chosen

¹https://github.com/google/edward2/

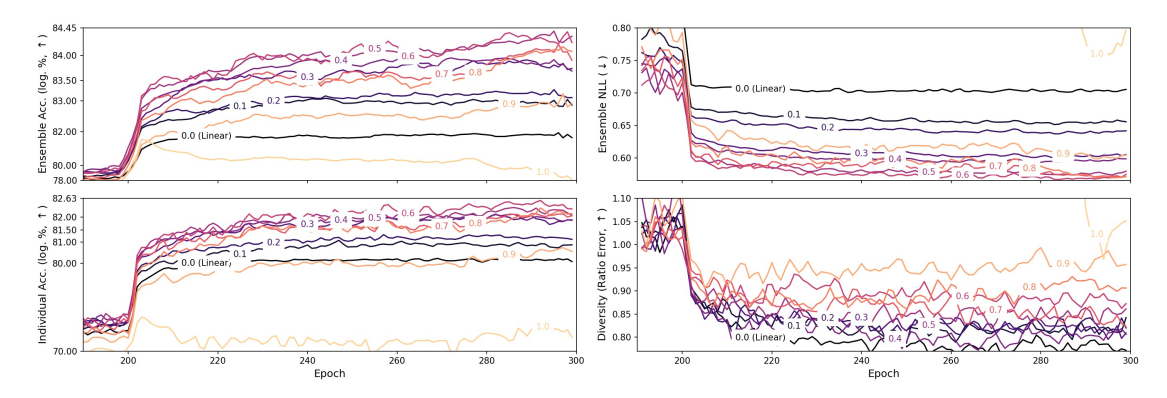


Figure 12: **Training dynamics**. Higher probability p of binary mixing via patches increases diversity (lower right), and also individual accuracy (lower left) but only up to p = 0.6. At this intermediate value, we obtain best ensemble performances, in terms of accuracy (upper left) or uncertainty estimation (upper right). b = 2, r = 3, $\alpha = 3$ with WRN-28-10 on CIFAR-100.

in the whole dataset, and not only inside the current batch². Moreover, $\mathcal{M}_{\text{Cut-MixMo}}$ modifies by $\mathbb{1}_{\mathcal{M}}$ the visible part from mask $\mathbb{1}_m$ (of area λ). We thus modify targets accordingly: $(\lambda' y_i + (1-\lambda') y_k, y_j)$ where $\lambda' = \frac{\sum \mathbb{1}_m \odot \mathbb{1}_{\mathcal{M}}}{\sum \mathbb{1}_{\mathcal{M}}}$. To fully benefit from b, we force the repeated x_i to remain predominant in its b appearances: *i.e.*, we swap x_i and x_k if $\lambda' < 0.5$. We see CutMix as a perturbation on the main batch sample.

Distributional uncertainty measures help when there is a mismatch between train and test data distributions. Thus [43] introduced **CIFAR-100-c** on which **AugMix** performs best. AugMix sums the pixels from a chain of several augmentations and is complementary to our approach in features. We use default parameters³: the severity is set 3, the mixture's width to 3 and the mixture's depth to 4. We exclude operations in AugMix which overlap with CIFAR-100-c corruptions: thus, [equalize, posterize, rotate, solarize, shear_x, shear_y, translate_x, translate_y] remain. We disabled the Jensen-Shannon Divergence loss between predictions for the clean image and predictions for the same image AugMix augmented: that would otherwise triple the training time.

6.5. Training dynamics

Fig. 12 showcases training dynamics for probability $p \in [0,1]$ of binary mixing via patches (see Section 4.3.2). For p=0, we recover Linear-MixMo; for p=0.5, we recover our standard Cut-MixMo. Diversity is measured by the ratio-error, the ratio between the number of samples on which only one of the two predictor is wrong, divided by the number of samples on which they are both wrong. It is positively correlated with p. However, individual accuracies first increase with p until p=0.6, then the tendency is reversed. We speculate this is caused mainly by increased

train-test distribution gap and by underfitting. Overall, best ensemble performances in terms of accuracy and uncertainty estimation are obtained with $p \in [0.5, 0.6]$. We note that the performance gap is stable along training. Moreover, here uncertainty estimation is measured with *Negative Log-Likelihood* (NLL) (before temperature scaling): the difference between Linear-MixMo and Cut-MixMo is similar to the one in NLL $_c$ (after temperature scaling).

6.6. Mixing sample data augmentation

We have drawn inspiration from MSDA techniques to design our mixing block \mathcal{M} . In particular, Section 4.3.2 compared different \mathcal{M} based on recent papers. Fig. 13 provides the reader a visual understanding of their behaviour, which we explain below.

MixUp [117] linearly interpolates between pixels values: $m_x(x_i, x_k, \lambda) = \lambda x_i + (1-\lambda)x_k$. The remaining methods fall under the label of **binary MSDA**: $m_x(x_i, x_k, \lambda) = 0$



Figure 13: Common MSDA procedures with $\lambda = 0.5$.

²Following https://github.com/ildoonet/cutmix
³https://github.com/google-research/augmix/
blob/master/cifar.py

 $\mathbb{1}_m \odot x_i + (\mathbb{1} - \mathbb{1}_m) \odot x_k$ with $\mathbb{1}_m$ a mask with binary values $\{0,1\}$ and area of ratio λ . They diverge in how this mask is created. The horizontal concatenation, also found in [92], simply draws a vertical line such that every pixel to the left belongs to one sample and every pixel to the right belongs to the other. Similarly, we define a vertical concatenation with an horizontal line. PatchUp [23] adapted DropBlock [31]: a canvas C of patches is created by sampling for every spatial coordinate from the Bernoulli distribution Ber(λ') (where λ' is a recalibrated value of λ): if the drawn binary value is 1, a patch around that coordinate is set to 1 on the final binary mask $\mathbb{1}_m$. PatchUp was designed for in-manifold mixing with a different mask by channels. However, duplicating the same 2D mask in all channels for \mathcal{M} performs better in our experiments. **FMix** [37] selects a large contiguous region in one image and pastes it onto another. The binary mask is made of the top- λ percentile of pixels from a low-pass filtered 2D map G drawn from an isotropic Gaussian distribution. CowMix [26, 27] selects a cow-spotted set of regions, and is somehow similar to FMix with a Gaussian filtered 2D map G. CutMix [114] was inspired by CutOut [19]. Formally, we sample a square with edges of length $R\sqrt{\lambda}$, where R is the length of an image edge. Note that this sometimes leads to non square rectangles when the initially sampled square overlaps with the edge from the original image. We adjust our λ a posteriori to fix this boundary effect. Regarding the hyper-parameters, we use in \mathcal{M} those provided in the seminal papers, except for sampling of κ where we set $\alpha = 2$ in all setups.

6.7. Hyper-parameter α

In Fig. 14, we study the impact of different values of α , parameterizing the sampling law for $\kappa \sim \text{Beta}(\alpha,\alpha)$. For high values of α , the interval of κ narrows down around 0.5. Diversity is therefore decreased: we speculate this is because we do not benefit anymore from lopsided updates. The opposite extreme, when $\alpha{=}1$, is equivalent to uniform distribution between 0 and 1. Therefore diversity is increased, at the cost of lower individual accuracy due to less stable training. For simplicity, we set $\alpha{=}2$. Manifold-Mixup [101] selected the same value on CIFAR-100. However, this value could be fine tuned on the target task: e.g. in Fig. 14, $\alpha{=}4$ seems to perform best for Cut-MixMo on CIFAR-100 with WRN-28-10 with $r{=}3$, $p{=}0.5$ and $b{=}2$.

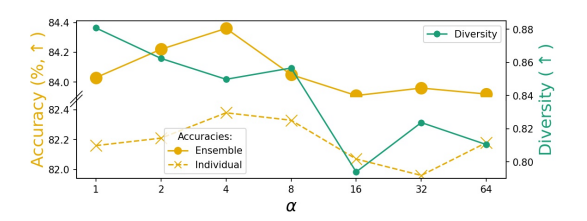


Figure 14: **Diversity/accuracy** as function of α .

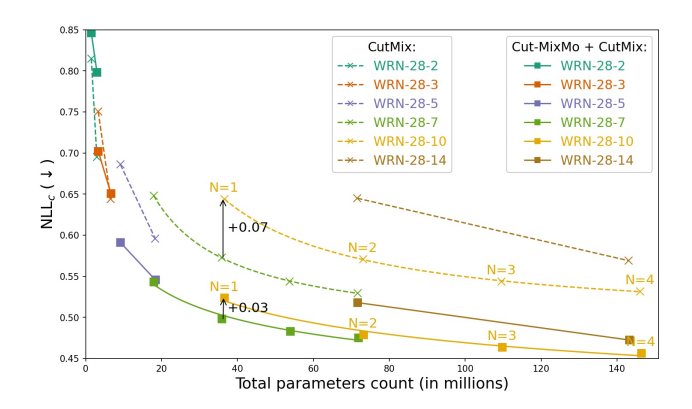


Figure 15: **Ensemble effectiveness** (NLL_c/#params). We slide the width in WRN-28-w and numbers of members N. CutMix data augmentation. Interpolations through power laws [67] when more than 2 points are available.

6.8. Ensemble of Cut-MixMo with CutMix

Fig. 15 plots performance for different widths w in WRN-28-w and varying number of ensembled networks N: two vertically aligned points have the same parameter budget. Indeed, the total number of parameters in our architectures has been used as a proxy for model complexity, as in [15, 67]. We compare ensembling with CutMix rather than standard pixels data augmentation, as previously done in Fig. 6 from Section 4.6. For a fixed memory budget, a single network usually performs worse than an ensemble of several medium-size networks: we recover the **Memory Split Advantage** even with CutMix. However, Cut-MixMo challenges this by remaining closer to the lower envelope. In other words, parameters allocation (more networks or bigger networks) has less impact on results. This is due to Cut-MixMo's ability to better use large networks.

In Table 9, we summarize several experiments on CIFAR-100. Among other things, we can observe that large vanilla networks tend to gain less from ensembling [67]: e.g. 2 vanillas WRN-28-10 (83.17% Top1, 0.668 NLL_c) do not perform much better than 2 WRN-28-7 (82.94%, 0.673). This remains true even with CutMix: (85.74%,0.571) vs. (85.52%, 0.573). We speculate this is related to wide networks' tendency to converge to less diverse solutions, as studied in [71]. Contrarily, MixMo improves the ensembling of large networks, with (86.04%, 0.494)vs. (85.50%, 0.517) on the same setup. When additionally combined with CutMix, we obtain state of the art (86.63%, 0.479) vs. (85.90%, 0.498). This demonstrates the importance of Cut-MixMo in cooperation with standard pixels data augmentation. It attenuates the drawbacks from overparameterization This is of great importance for practical efficiency: it modifies the optimal network width for realworld applications.

Table 9: Summary: WRN-28-w on CIFAR-100. b = 4.

Width	Approach	1-1	Net	2-N	lets	Linear-	MixMo	Cut-N	IixMo	2-Cut-N	/lixMos
w	CutMix	-	✓	-	✓	-	✓	-	✓	-	√
2	Top1 NLL _c # params	76.44 0.921 1.4	78.06 0.815 8M	79.16 0.776 2.9	80.81 0.695 5M	75.82 0.841	76.36 0.824 1.49	75.66 0.824 9M	75.17 0.846	76.98 0.7661 2.99	76.11 0.798 9M
3	Top1 NLL _c # params	77.95 0.862 3.3	80.70 0.750 1M	80.85 0.738 6.6	83.14 0.644 2M	78.51 0.760	80.74 0.696 3.33	79.81 0.693 3M	79.85 0.702	80.78 0.635 6.60	81.20 0.650 6M
4	Top1 NLL _c # params	78.84 0.824 5.8	81.55 0.711 7M	81.48 0.711 11.7	83.93 0.609 74M	80.43 0.712	81.66 0.656 5.89	81.68 0.646 9M	81.69 0.635	82.57 0.590 11.7	82.58 0.588 '9M
5	Top1 NLL _c # params	79.75 0.813 9.1	82.55 0.686 6M	82.18 0.693 18.3	84.60 0.596 32M	80.95 0.703	83.06 0.617 9.19	83.11 0.598 9M	83.34 0.591	83.97 0.549 18.3	84.31 0.546 9M
7	Top1 NLL _c # params	81.14 0.764 17.9	83.71 0.648 92M	82.94 0.673 35.8	85.52 0.573 85M	82.4 0.675	84.51 0.581 17.9	84.32 0.562 7M	84.94 0.543	85.50 0.516 35.9	85.90 0.498 94M
10	Top1 NLL _c # params	81.63 0.750 36.5	84.05 0.644 53M	83.17 0.668 73.0	85.74 0.571 07M	83.08 0.656	85.47 0.558 36.6	85.40 0.535 0M	85.77 0.524	86.04 0.494 73.2	86.63 0.479 21M
14	Top1 NLL _c # params	82.01 0.730 71.5	84.31 0.645 55M	83.47 0.656 143	85.80 0.569 .1M	83.79 0.648	86.05 0.545 71.6	85.76 0.527 64M	86.19 0.518	86.58 0.488 143.2	87.11 0.473 28M

6.9. Pseudo Code

Finally, the pseudo-code in Algorithm 1 describes the procedure behind Cut-MixMo with ${\cal M}=2.$

```
Algorithm 1: Procedure for Cut-MixMo with M=2 subnetworks
   /* Setup
   Parameters: First convolutions \{c_0, c_1\}, dense layers \{d_0, d_1\} and core network C, randomly initialized.
   Input: Dataset D = \{x_i, y_i\}_{i=1}^{|D|}, probability p of applying binary mixing via patches, reweighting coefficient r,
             concentration parameter \alpha, batch size b_s, batch repetition b, optimizer g, learning rate l_r.
   /* Training Procedure
                                                                                                                                                      */
1 for epoch from 1 to #epochs do
        for step from 1 to \frac{|D| \times b}{b_s} do | /* Step 1: Batch creation
2
             Randomly select \frac{b_s}{b} samples
                                                                                                                                     // Sampling
3
             Duplicate these samples b times to create batch \{x_i, y_i\}_{i \in B} of size b_s
4
                                                                                                                     // Batch repetition
             Randomly shuffle B with \pi to create \{(x_i, x_j), (y_i, y_j)\}_{i \in B, j = \pi(i)}
                                                                                                                                   // Shuffling
5
             /* Step 2: Define the mixing mechanism at the batch level
                                                                                                                                                      */
             Sample 1_{binary} \sim Ber(p) from Bernoulli distribution // Whether we apply binary or linear
              mixing
                                                        // Whether the first input is inside or outside the
             Sample 1_{outside} \sim Ber(0.5)
7
              rectangle
             /* Step 3:
                                  Forward and loss
                                                                                                                                                      */
             for i \in B do
8
                  Sample \kappa_i \sim \text{Beta}(\alpha, \alpha)
                  l_i^0 = c_0(x_i) and l_i^1 = c_1(x_{\pi(i)})
10
                  if 1_{binary} then
11
                       Sample \mathbb{1}_{\mathcal{M}} a rectangular binary mask with average \kappa_i (as in CutMix)
12
                       if 1_{outside} then
13
                           1_{\mathcal{M}} \leftarrow 1 - 1_{\mathcal{M}}
                                                                 // Permute the rectangle and its complementary
14
                          \kappa_i \leftarrow 1 - \kappa_i
15
                      l_i = 2 \left[ \mathbb{1}_{\mathcal{M}} \odot l_0 + (\mathbb{1} - \mathbb{1}_{\mathcal{M}}) \odot l_1 \right]
                                                                                                                // Apply binary mixing
16
17
                   l_i = 2 \left[ \kappa_i l_0 + (1 - \kappa_i) l_1 \right]
                                                                                                  // Apply linear interpolation
18
                  Extract features f_i \leftarrow \mathcal{C}(l_i) from core network
19
                 Compute predictions \hat{y}_i^0 \leftarrow d_0(f_i) and \hat{y}_i^1 \leftarrow d_1(f_i)

Compute weights w_i \leftarrow 2\frac{\kappa_i^{1/r}}{\kappa_i^{1/r} + (1-\kappa_i)^{1/r}}

Compute loss \mathcal{L}_i \leftarrow w_i \mathcal{L}_{\text{CE}}\left(y_i, \hat{y}_i^0\right) + (2-w_i) \mathcal{L}_{\text{CE}}\left(y_{\pi(i)}, \hat{y}_i^1\right)
20
21
22
23
```

24